Received: 14 December 2017 | Accepted: 16 July 2018

DOI: 10.1111/2041-210X.13068

RESEARCH ARTICLE

Methods in Ecology and Evolution BRITISH ECOLOGICAL SOCIETY

Estimating recruitment from capture–recapture data by modelling spatio-temporal variation in birth and age-specific survival rates

Richard B. Chandler[1] | Kristin Engebretsen[1] | Michael J. Cherry[2] | Elina P. Garrison[3] | Karl V. Miller[1]

[1]Warnell School of Forestry and Natural Resources, University of Georgia, Athens, Georgia, USA

[2]Department of Fish and Wildlife Conservation, Virginia Tech, Blacksburg, Virginia, USA

[3]Florida Fish and Wildlife Conservation Commission, Tallahassee, Florida, USA

Correspondence
Richard B. Chandler
Email: rchandler@warnell.uga.edu

Funding information
Florida Fish and Wildlife Conservation Commission

Handling Editor: Diana Fisher

Abstract

1. Understanding the factors influencing recruitment in animal populations is an important objective of many research and conservation programmes. However, evaluating hypotheses is challenging because recruitment is the outcome of birth and survival processes that are difficult to directly observe. Capture–recapture is the most general framework for estimating recruitment in the presence of observation error, but existing methods ignore the underlying birth and survival processes, as well as age effects and spatial variation in vital rates.
2. We present an individual-based, spatio-temporal model that can be fit to capture–recapture data to draw inferences on the birth and survival processes governing recruitment dynamics. The number, dates, and spatial distribution of births are modelled as outcomes of a point process, and survival is modelled using a failure time approach. Survival parameters can be modelled as functions of individuals traits and time-varying, spatial covariates. Continuous- and discrete-time formulations are possible. We demonstrate the model using 7 months of camera data collected on white-tailed deer *Odocoileus virginianus* fawns in Big Cypress National Preserve. Spot patterns were used to individually identify 28 fawns, detected 1,454 times between December 1, 2015 and July 1, 2016.
3. A total of 37 (95% CI: 30–49) fawns were born, of which 16 (95% CI: 10–23) survived 180 days to the recruitment age. Mean parturition date was February 14 (95% CI: February 6–February 22), much earlier than in more temperate parts of the species' range, but coinciding with the dry season in southern Florida. We found little evidence that mortality rates decreased with age, but the estimate of the age effect was imprecise. In contrast, we found strong evidence that encounter rates were age-specific and increased rapidly over the first month of life as fawns became more mobile.
4. Our case study demonstrates the potential of this new model for advancing knowledge of spatial population dynamics by providing insights into the birth and juvenile survival processes that influence recruitment. Because the model can be applied to data from noninvasive survey methods such as camera trapping, it is

possible to apply it at broad spatial scales to understand how environmental variables and predator communities influence recruitment.

KEYWORDS
birth-death process, camera trapping, individual-based models, spatial capture–recapture, spatial demography, spatio-temporal point process, white-tailed deer

1 | INTRODUCTION

Recruitment is a fundamental process of interest in studies of population dynamics, and many conservation organizations monitor recruitment to inform their management actions (Chitwood et al., 2017; USFWS, 2017; Williams, Nichols, & Conroy, 2002). Broadly defined, recruitment is the process by which new individuals enter a population, but in most cases, interest lies in *in situ* recruitment of individuals that were born into the population and survived to a specified age, such as age of sexual maturity (Nichols & Pollock, 1990; Schaub, Ullrich, Knötzsch, Albrecht, & Meisser, 2006). Evaluating hypotheses about *in situ* recruitment (hereafter, recruitment) is challenging because it is the outcome of birth and survival processes that occur continuously in time and are difficult to directly measure.

Numerous capture–recapture methods have been developed to estimate recruitment when imperfect detection makes it impossible to directly observe (Jolly, 1965; Schwarz & Arnason, 1996; Seber, 1965). However, these models are designed for data that are assumed to arise from instantaneous sampling, or for scenarios in which it is safe to assume population closure such that recruitment occurs between, but not during, sampling occasions (Pollock, 1982; Williams et al., 2002). These assumptions may be reasonable for birth pulse populations where the breeding season is relatively short and synchronized, or when reproduction and mortality rates are negligible during the sampling period. However, for many species, the breeding season is long and characterized by high juvenile mortality, making the closure assumption problematic.

Another limitation of many capture–recapture approaches to recruitment estimation is that they do not accommodate age effects. If they do, they assume that age is known precisely, which is rarely possible (Crosbie & Manly, 1985; Stokes, 1984). Ignoring age data makes it difficult to draw inferences on age-specific survival rates, which is problematic because survival rates of young individuals can vary dramatically with age, and recruitment may be influenced by this variation more than it is by the number of individuals born (Pradel & Lebreton, 1999). Estimating age-related variation in survival is therefore desirable, but capture probability can also change with age, and conventional survival estimators will be biased if age-related variation in capture probability is ignored (Matechou, Pledger, Efford, Morgan, & Thomson, 2013; Pollock, 1981).

Of the capture–recapture models that do allow for age effects (Crosbie & Manly, 1985; Pollock, 1981; Stokes, 1984), no spatially explicit methods exist. Instead, most models are designed for a single population in a homogeneous environment (Pradel, 1996), or for a metapopulation consisting of a small number of subpopulations connected by dispersal (Lebreton, Hines, Pradel, Nichols, & Spendelow, 2003; Sanderlin, Waser, Hines, & Nichols, 2012). This is an important limitation because vital rates often depend on age and location, and ecologists are increasingly interested in evaluating hypotheses about the effects of spatial heterogeneity in the environment on demographic processes (Godsoe, Jankowski, Holt, & Gravel, 2017; Gurevitch, Fox, Fowler, Graham, & Thomson, 2016; Merow et al., 2014).

Recently developed spatial capture–recapture (SCR) models enable inference on spatial variation in density and detection parameters (Borchers & Efford, 2008; Efford, 2004; Royle, Chandler, Sollmann, & Gardner, 2014), but the majority of these models assume demographic closure (i.e., no reproduction or mortality). Open population SCR models have been developed (Gardner, Reppucci, Lucherini, & Royle, 2010; Raabe, Gardner, & Hightower, 2013; Schaub & Royle, 2014) and offer potential for advancing knowledge of spatial population dynamics. However, as with nonspatial models, existing models do not allow for insights into the underlying birth and juvenile survival processes that determine recruitment, and to date, they have not incorporated age effects.

The purpose of this paper is to present a statistical modelling framework that can be used to estimate the number of individuals recruited into a population by modelling spatial and temporal variation in birth rates and juvenile survival. The model also allows for mortality rates and captures probabilities, or encounter rates, to depend on age. We demonstrate the utility of this approach using data from a white-tailed deer *Odocoileus virginianus* population of substantial conservation interest because it serves as the prey base for the endangered Florida panther *Puma concolor coryi*.

2 | MODEL

2.1 | Ecological process models

We develop a hierarchical model with a spatio-temporal point process to describe the number, times, and locations of births. Spatio-temporal point process models are well-suited to ecological data because they allow for population-level inference from individual-level data on the locations and times of events such as birth or mortality (Cox & Isham, 1980; Diggle, 2013; González, Rodríguez-Cortés, Cronie, & Mateu, 2016; Rathbun & Cressie, 1994). However, standard point process models require data on all individuals in the

population, which is typically impossible to achieve because many animals go undetected as a result of spatial sampling and imperfect detection. We deal with this obstacle in Section 2.2 by using a thinned point process model for the capture–recapture data. In addition to the birth and detection processes, survival is modelled using a failure time approach, in which lifetime (i.e., the duration of an individual's life) is modelled as a random variable (Cox & Oakes, 1984). Recruitment is estimated as the number of individuals that live longer than a prescribed "recruitment age." The ecological state variables of interest are:

B	births during time frame $\mathcal{T} \subset \mathbb{R}$ in spatial region $\mathcal{S} \subset \mathbb{R}^2$
$(t_1, \ldots, t_B) \in \mathcal{T}$	times of birth
$(\boldsymbol{s}_1, \ldots, \boldsymbol{s}_B) \in \mathcal{S}$	locations of birth
$(l_1, \ldots, l_B) \in (0, \infty)$	lifetimes
$a_1(t), \ldots, a_B(t)$	ages at time t
$N(t)$	abundance at time t
$R(t)$	recruits alive at time t

The last three variables are functions of the first four. The issue of defining $\mathcal{T}$ and $\mathcal{S}$ is discussed in Section 2.2.

2.1.1 | Birth process

In some cases, the location of birth might depend on time, calling for a model of the joint distribution $p(\{(\boldsymbol{s}_i, t_i)\}_{i=1}^{B}, B|\boldsymbol{\Theta})$. This distribution is determined by $\gamma(\boldsymbol{s}, t, \boldsymbol{\Theta}) \geq 0$, the spatio-temporal intensity function describing the expected number of births at location $\boldsymbol{s}$ and time t. Note that, in keeping with conventional point process notation, $\boldsymbol{s}$ and t without subscripts reference space and time, whereas $\boldsymbol{s}_i$ and t_i indicate the location and time of a particular birth event. The intensity function also determines the expected number of births in $\mathcal{S} \times \mathcal{T}$, according to:

$$E(B) = \Gamma = \int_{\mathcal{T}} \int_{\mathcal{S}} \gamma(\boldsymbol{s}, t, \boldsymbol{\Theta}) \, \mathrm{d}\boldsymbol{s}\mathrm{d}t \tag{1}$$

The intensity function can depend on spatial, temporal, and spatio-temporal covariates. Random effects could be incorporated too, but here we focus on fixed effects, which can be modelled as a linear combination on a link scale: $g(\gamma(\boldsymbol{s}, t, \boldsymbol{\Theta})) = \boldsymbol{v}'(\boldsymbol{s}, t)\boldsymbol{\beta}$. For example, habitat-specific birth times could be modelled using a log-linear model with an interaction between an environmental covariate $v(\boldsymbol{s})$ and time: $\log(\gamma(\boldsymbol{s}, t, \boldsymbol{\Theta})) = \beta_0 + \beta_1 v(\boldsymbol{s}) + \beta_2 t + \beta_3 v(\boldsymbol{s})t$. Regardless of the chosen intensity function, the conditional (on B) probability distribution of $(\boldsymbol{s}_i, t_i)$ is:

$$p((\boldsymbol{s}_i, t_i)|\boldsymbol{\Theta}) = \gamma(\boldsymbol{s}_i, t_i, \boldsymbol{\Theta})/\Gamma$$

Assuming all points in the pattern are conditionally independent of one another, the joint probability distribution of the point pattern is

$$p(\{(\boldsymbol{s}_i, t_i)\}_{i=1}^{B}, B|\gamma(\boldsymbol{s}, t|\boldsymbol{\Theta})) = p(B) \prod_{i=1}^{B} p((\boldsymbol{s}_i, t_i)|\boldsymbol{\Theta}) \tag{2}$$

A Poisson distribution is often used for $p(B)$, but to facilitate model fitting, we use data augmentation (Royle, 2009) to fix the dimensions of the parameter space by setting $M \gg B$ and adopting a binomial model: $p(B) = \mathrm{Bin}(M, \psi)$, or equivalently a set of latent variables $p(b_i) = \mathrm{Bern}(\psi)$ for $i = 1, \ldots, M$, with $B = \sum_{i=1}^{M} b_i$. Regardless, from here onward, all individual-specific variables will have an upper index of M instead of B. The parameter ψ is a function of the expected number of births according to $\psi = \Gamma/M$. However, it is also possible to place a prior directly on ψ, and then model the birth times and locations independently as described below.

If the times and locations of births are independent, the model can be simplified by factoring the joint distribution into the product of densities for the two conditional point process models and the indicator variable b_i:

$$p((\boldsymbol{s}_i, t_i, b_i)|\boldsymbol{\Theta}) = p(\boldsymbol{s}_i|\gamma(\boldsymbol{s}, \boldsymbol{\theta}))p(t_i|\gamma(t, \boldsymbol{\vartheta}))p(b_i|\psi)$$

where $\boldsymbol{\Theta} = (\boldsymbol{\theta}, \boldsymbol{\vartheta}, \psi)$. Unlike the intensity function of the joint distribution, intensities of the conditional point process distributions do not need to integrate to $E(B)$. Instead, they simply describe the distributions of the M points (Diggle, 2013). The probability densities of the independent conditional point processes are found by normalizing, eg: $p(\boldsymbol{s}_i|\gamma(\boldsymbol{s}, \boldsymbol{\theta})) = \gamma(\boldsymbol{s}_i, \boldsymbol{\theta}) / \int_{\mathcal{S}} \gamma(\boldsymbol{s}, \boldsymbol{\theta}) \, \mathrm{d}\boldsymbol{s}$.

Several options exist for specifying the conditional distributions of birth times and locations. For birth pulse populations, a Gaussian kernel (or a mixture of kernels) could be used for the birth times, leading to $p(t_i|\gamma(t, \boldsymbol{\vartheta})) = \mathrm{Norm}(\bar{t}, \varsigma^2)$ where $\boldsymbol{\vartheta} = (\bar{t}, \varsigma^2)$. For birth flow populations, a uniform distribution could be used in place of the normal distribution. If there are no hypotheses about how density varies in space, a natural starting point for the conditional distribution of birth locations would be $p(\boldsymbol{s}_i|\gamma(\boldsymbol{s}, \boldsymbol{\theta})) = \mathrm{Unif}(\mathcal{S})$. Otherwise, an arbitrary spatial intensity function with covariates could be used and then normalized to obtain the probability density.

2.1.2 | Survival

Mortality rate can depend on the time of birth, the location of birth, the age of an individual, and other factors such as temporally varying environmental conditions. Drawing inferences about these processes can be accomplished using a spatial survival model defined in terms of l_i, the lifetime of individual i. Standard lifetime distributions include the exponential and Weibull distributions, but other parametric distributions suitable for positive, continuous variables could be used. Alternatively, semiparametric models could be constructed from a hazard function describing the instantaneous rate of mortality, conditional on surviving to age a, where an individual's age at time t is denoted by $a_i(t) = t - t_i$.

Dropping the time and individual indexes for clarity, we denote the hazard function by $\Omega(a)$. Under the exponential model, the hazard does not change with age: $\Omega(a) = \Omega = 1/\omega_1$, whereas the age-dependent hazard of the Weibull distribution is $\Omega(a) = \omega_0/\omega_1(a/\omega_1)^{\omega_0 - 1}$. When $\omega_0 = 1$, the Weibull distribution is equivalent to the exponential distribution. When $\omega_0 < 1$, the hazard

decreases with age. Many other forms of the hazard are possible but they must meet the conditions $\Omega(a) > 0$ and $\int_0^\infty \Omega(a)\,da = \infty$ to ensure that lifetime is finite (Cox & Oakes, 1984). The probability of surviving to age a is known as the survivorship function, which is based on the cumulative hazard: $\Phi(a) = \exp(-\int_0^a \Omega(a)\,da)$. The lifetime probability distribution is the probability of surviving to, and dying at, age l: $p(l) = \Phi(l)\Omega(l)$.

The model can be generalized by allowing the hazard to depend on the time and location of birth. Individual-specific, time-varying covariates could be accommodated using a proportional hazards model such as

$$\Omega(a_i(t), \boldsymbol{s}_i, t_i) = \Omega_0(a_i(t)) \exp(\boldsymbol{w}'(\boldsymbol{s}_i, t_i)\boldsymbol{\beta})$$

where $\Omega_0(a_i(t))$ is the baseline hazard rate, which could be one of the models mentioned above. The spatio-temporal covariates $\boldsymbol{w}(\boldsymbol{s}_i, t_i)$ serve to shift the baseline hazard by a constant determined by the regression coefficients $\boldsymbol{\beta}$.

2.1.3 | Abundance, density and recruitment

Because birth and mortality events occur continuously in time, abundance and density also vary continuously. Abundance is simply the number of individuals alive at time t, which we define as $N(t) = \sum_{i=1}^{M} z_i(t)$ where

$$z_i(t) = \begin{cases} 1 & \text{if } t_i \le t < d_i \text{ and } b_i = 1 \\ 0 & \text{otherwise} \end{cases} \quad (3)$$

with $d_i = t_i + l_i$ being the time of mortality. Letting $|\mathcal{S}|$ denote the area of the spatial region, density is given by $D(t) = N(t)/|\mathcal{S}|$. It is important to note that $N(t)$ is the abundance of individuals born in $\mathcal{T}$, which may be a subset of the population if, for example, only a single cohort of individuals is being studied. Multiple cohorts could be studied, using a multimodal intensity function for the birth times.

The number of recruits alive at time t is the number of individuals born during $\mathcal{T}$ whose age is greater than the prescribed recruitment age, $\tilde{a}$, which could be the age at maturity or some other age that suits the research or monitoring objective. Regardless, the abundance of recruits at time t is given by the following:

$$R(t) = \sum_{i=1}^{M} I(a_i(t) \ge \tilde{a}) z_i(t)$$

where $I(\cdot)$ is the indicator function returning 1 if the argument is true and zero otherwise.

2.2 | Model for the capture–recapture data

The primary challenge facing research on recruitment is that the state variables cannot be directly observed because sampling from a collection of points or plots during a finite time interval results in censoring as well as failure to detect some of the individuals in the population of interest. Censoring occurs when a continuous random variable is not directly observed, but is known to lie within an interval. In our model, the lifetimes of the detected individuals are right-censored, and the birth dates may be interval-censored if age information is available to determine minimum and maximum birth dates. To deal with the censoring and imperfect detection obstacles, we develop an observation model to describe how the data arise conditional on the latent state variables.

The data may be recorded in either discrete time intervals or in continuous time within the sampling period denoted by $\mathscr{T}$. Although the discrete time models are much more common, we begin with a continuous model because we formulated the state process in continuous time, and because continuous-time data are becoming more common with the widespread use of camera trapping, acoustic telemetry, and similar technologies (Borchers, Distiller, Foster, Harmsen, & Milazzo, 2014; Dorazio & Karanth, 2017). Discrete-time models are discussed in Section 3.2. Let $\ddot{\boldsymbol{t}}_{ij}$ represent the vector of detection times for individual i ($i = 1, \ldots, n$) at detector j ($j = 1, \ldots, J$). We model the detection times as outcomes of a temporal point process that is conditional on the distance between activity centres and detectors. Detectors may be physical traps or noninvasive devices such as camera traps. The following is a list of the data variables that may be available:

$y_{i1}, \ldots, y_{iJ}$	number of captures of individual i at each detector
$(\ddot{t}_{ij1}, \ldots, \ddot{t}_{ijy_{ij}}) \in \mathscr{T}$	times of capture for individual i at detector j
$r_1, \ldots, r_n$	minimum and maximum birth times for each detected individual
$\boldsymbol{x}_1, \ldots, \boldsymbol{x}_J$	detector locations
$\boldsymbol{w}_1, \ldots, \boldsymbol{w}_n$	individual-level, potentially time-varying, covariates (e.g., age, sex) recorded for each detection event
$\boldsymbol{v}(s, t)$	spatio-temporal covariates (e.g., elevation, temperature, forest type)

To facilitate model fitting, the capture frequencies (y_{ij}) are augmented with $M - n$ rows of zeros. The individual-level covariates are augmented with missing values, and must be imputed during model fitting (Royle, 2009; Royle, Dorazio, & Link, 2007).

Let $\lambda(\boldsymbol{s}_i, \boldsymbol{x}_j, t)$ denote the temporal intensity function at detector $\boldsymbol{x}_j$ for an individual with activity centre at $\boldsymbol{s}_i$. One possible model is as follows: $\lambda(\boldsymbol{s}_i, \boldsymbol{x}_j, t) = \lambda_0 \exp(-\|\boldsymbol{s}_i - \boldsymbol{x}_j\|^2/(2\sigma^2))z_i(t)$, which ensures that the detection rate decreases with distance between activity centres and detectors, and is zero if the individual is not alive at time t (i.e., $z_i(t) = 0$). The expected number of detections of individual i at $\boldsymbol{x}_j$ is given by $E(y_{ij}) = \Lambda_{ij} = \int_{\mathscr{T}} \lambda(\boldsymbol{s}_i, \boldsymbol{x}_j, t)\,dt$. If y_{ij} is Poisson and the times of detection are independent, the joint probability of the temporal point process is given by:

$$\begin{aligned} p(\ddot{\boldsymbol{t}}_{ij}, y_{ij} \mid \lambda(\boldsymbol{s}_i, \boldsymbol{x}_j, t), z_i(t)) &= p(\ddot{\boldsymbol{t}}_{ij} \mid y_{ij}) p(y_{ij}) \\ &= \left\{ \prod_{m=1}^{y_{ij}} \frac{\ddot{t}_{ijm}}{\Lambda_{ij}} \right\} \frac{\Lambda_{ij}^{y_{ij}} \exp(-\Lambda_{ij})}{y_{ij}!} \end{aligned}$$

More complicated models of capture probability can be constructed to allow for temporal effects or additional sources of individual heterogeneity. For example, home range size often increases with age during the early portion of an individual's life, and age effects could be modelled by allowing the spatial scale parameter σ to increase with age.

2.2.1 | Age data

In some cases, it might be possible to determine the age of an individual at the time of capture, thereby making it possible to treat some of the birth dates as data rather than as latent variables. However, because age is a continuous variable, and most aging methods are approximate, age is unlikely to be known exactly. Nonetheless, even approximate age information may be beneficial and there are several options for including these data. First, independent experiments could be conducted with individuals of known age to build predictive models of age based on morphology. This would make it possible to predict the age of individuals detected during capture–recapture studies, while accounting for uncertainty. A second option is to determine the minimum and maximum dates of birth for each individual, and use these ranges $\{r_1, ..., r_n\}$ as data in an interval-censored model. For example, the model $p(t_i|\gamma(t, \vartheta)) = \text{Norm}(\bar{t}, \varsigma^2)$ could be expanded to $p(\mathbf{r}_i|t_i)p(t_i|\gamma(t, \vartheta))$ where $p(\mathbf{r}_i|t_i) = I(r_{i1} \le t_i \le r_{i2})$. An application of this approach is discussed in Section 3.

2.2.2 | Defining the state-space

The state-space of $(\boldsymbol{s}_i, t_i)$ is $\mathcal{S} \times \mathcal{T}$, which must be defined as part of the analysis. As with closed-population SCR models, the spatial region $\mathcal{S}$ should include the population of interest and should be sufficiently large to ensure that the encounter rate is negligible for an individual whose activity centre (or birth site) is located near the boundary of the region. Smaller choices of $\mathcal{S}$ will result in undue truncation, causing upward bias in estimates of density. In contrast, making $\mathcal{S}$ larger will not affect density estimates (Royle et al., 2014, pp. 131–133). When specifying $\mathcal{T}$, the time interval during which births occur, the primary consideration is that the interval should be wide enough to include the birth times of all individuals that could be recruited during the time period of interest. As with $\mathcal{S}$, too narrow a definition of $\mathcal{T}$ will artificially truncate the point process and cause bias in estimates of birth times.

3 | APPLICATION TO THE FAWN DATA

3.1 | Methods

As part of a study of white-tailed deer (hereafter, deer) population dynamics in southern Florida, we deployed 60 passive infrared motion-sensor cameras with white flash (HCO Outdoor Products, Norcross, GA, USA; Figure 1) from December 1, 2015 to June 30, 2016. Cameras were placed in the North Addition Lands (Add Lands) unit of Big Cypress National Preserve. Forty of the cameras were placed along off-road vehicle (ORV) trails, although public ORV use was not allowed on most trails during the study period. Camera locations were chosen by placing a 725 m grid over a 6 × 5 km^2 rectangle in the Add Lands unit. The on-trail cameras were attached to the most suitable tree nearest to the designated grid cell point. The remaining 20 cameras were placed off-trail, approximately 250 m from the nearest on-trail camera. Camera density was chosen to balance goals of covering a large area while ensuring that individuals could be detected at multiple cameras within their home range (Royle et al., 2014, Ch. 10). Each camera was visited approximately once a month for camera maintenance and data download, and the vegetation around the camera was cleared to avoid visual obstruction and reduce false triggering of the camera.

Detected fawns were uniquely identified using their spot patterns, which are distinctive from birth until approximately 6 months

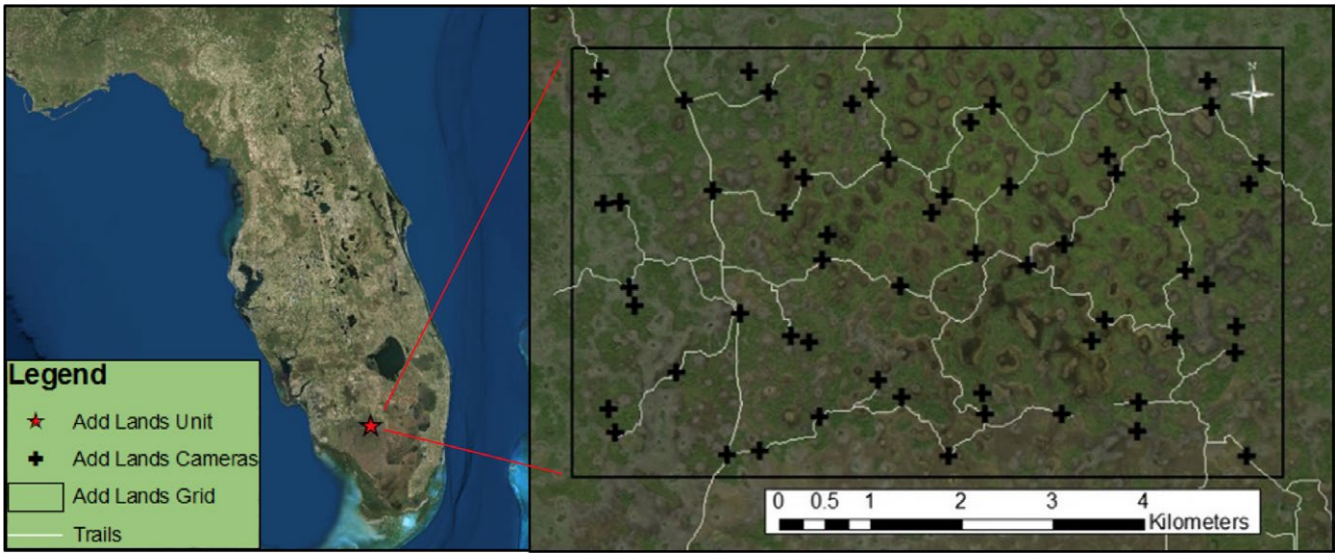

FIGURE 1 Study area and camera locations in Big Cypress National Preserve, Florida, USA

old. We studied the patterns of each fawn's spots on both sides and identified groupings of spots that were unique to the individual (Figure 2). We used a single-camera design throughout our study, with only one camera placed at each location in the grid. Studies focusing on spotted cats often utilize a two-camera system to capture an image of both flanks of the animal simultaneously. We used single-camera stations because we were interested in covering a broad geographical extent and because the adult portion of the deer population is unmarked. In spite of using a single camera at each station, we were able to visually confirm the identities of all detected fawns due to their tendency to spend substantial amount of time in front of the cameras, which allowed us to capture images of both flanks (Figure 2).

Because our model allows survival and detection rates to vary with age, information is needed about the ages of the detected individuals. However, as is the case with many wildlife species, fawn age could not be determined precisely from our camera data. To account for our uncertainty about the age of each detected individual, we created "birth date ranges" within which the actual birth date was believed to occur. To determine the birth date ranges, two experienced observers independently viewed images of each individual. Both observers had multiple seasons of experience capturing and collaring deer of various ages. Fawns detected very young (<10 days) and surviving many months helped provide a baseline for determining the birth date ranges of fawns that were detected less often. Factors considered in visual aging of fawns included size of fawn relative to the dam, head size and shape, brightness of spots, and length of hind leg relative to body size. The birth date ranges recorded by each observer were very similar, and minor discrepancies were resolved by using the earliest minimum and latest maximum birth date from the two observers.

We defined the recruitment age as 180 days old because this is the minimum age at which females could become sexually mature, and because it is often used as the recruitment age by state management agencies. However, the definition of recruitment age depends on the study objectives, and recruitment to any age can be estimated using our model.

Fawns were frequently detected in bursts of consecutive images as they lingered in front of the cameras. These clustered detections provide little information about the detection processes of interest and they violate the conditional independence assumption of the model, which states that detection times should be independent after accounting for the age of the fawn and the distance between activity centres and cameras (Section 2.2). We identified nonindependent detections by visually inspecting histograms of time differences between consecutive detections of each fawn at each camera. Histograms of the unthinned data were compared to histograms of data that were thinned using "independence thresholds" ranging from 10 to 60 min. For each threshold, we discarded detections of a fawn if it had been previously

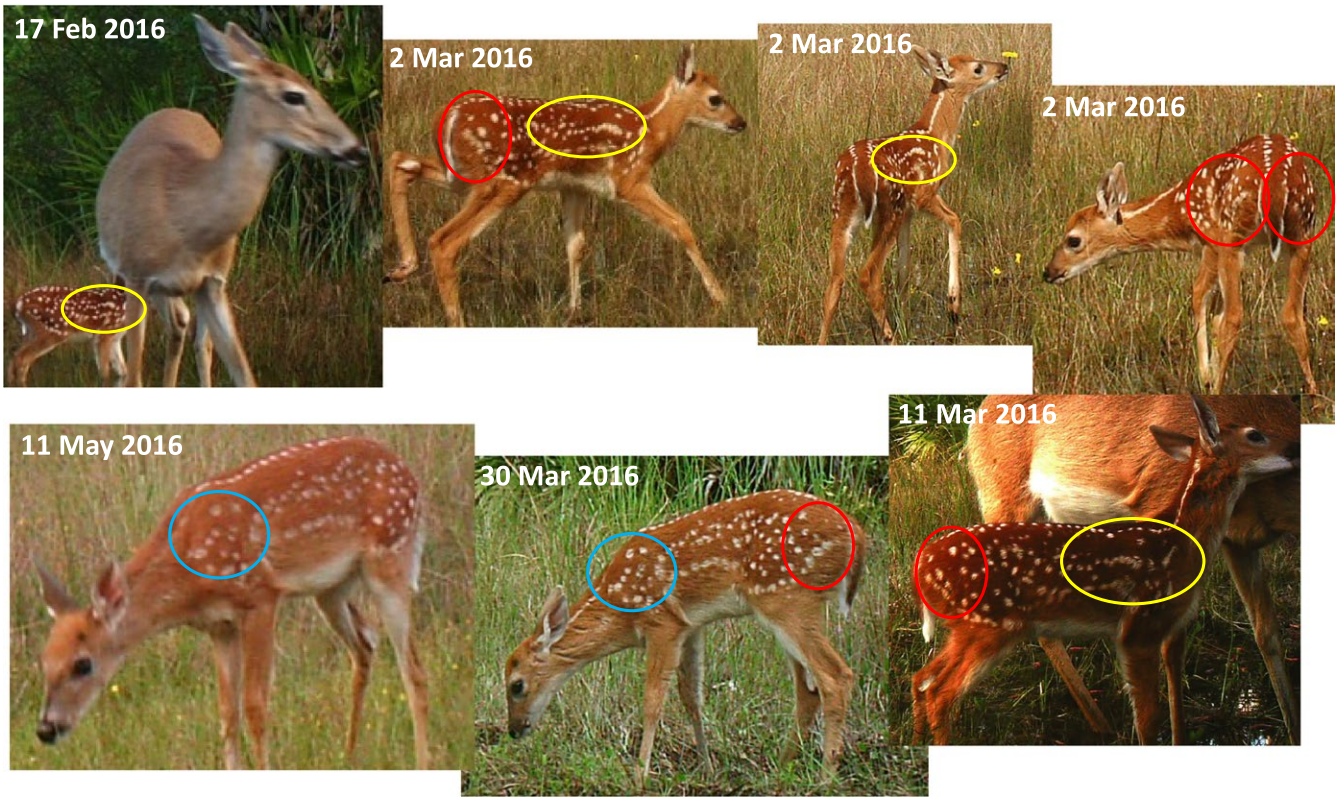

FIGURE 2 One of the 28 fawns detected during the study. All 28 individuals were uniquely identifiable because of distinctive spot patterns on left (blue ovals) and right (yellow ovals) flanks. We did not use a paired camera design but we were able to match spot patterns on both sides (red ovals) because fawns spent considerable time in front of the cameras

detected at the same camera within the threshold time period. Nonindependent detections should be evident by a high proportion of detections in the first time bin of the histogram. We selected the threshold that reduced the frequency of detections in the first bin to a level less than or equal to the highest frequency of detections in the other bins. We paired this visual inspection method with a Kolmogorov–Smirnov test to assess the null hypothesis that the time differences for the thinned data followed an exponential distribution, which would be true if the detection times are uniformly distributed in accordance with a homogeneous point process (Cox & Isham, 1980). This is a conservative test because our model is based on an inhomogeneous temporal point process that allows for some departures from the uniformity assumption. The Kolmogorov–Smirnov test was applied separately to each fawn-camera combination for which there were at least three detections.

3.2 | Model specification

We modelled birth times and locations independently because we had no reason to believe that they were dependent. Birth locations were modelled using a uniform distribution, $p(\boldsymbol{s}_i) = \text{Unif}(\mathcal{S})$, with $\mathcal{S}$ defined by a 700 m buffer around the camera array. The 700 m buffer was chosen to be large enough to ensure that fawns born farther away would not be detectable at our camera sites. The area of this polygon was 37.73 km^2. We defined the birthing time interval as $\mathcal{T} = [1, 150]$ spanning from December 1, 2015 to April 29, 2016, which is a subset of the sampling time interval $\mathcal{J} = [1, 213]$, spanning from December 1, 2015 to June 30, 2016. The birthing interval $\mathcal{T}$ was chosen by consulting the literature (Land, 1991), and by buffering the observed minimum and maximum birth date ranges by 30 days. Birth dates were modelled using an interval-censored normal distribution as described in Section 2.2.1. Because we used independent distributions for the birth times and locations, we modelled the data augmentation parameter with a $\psi = \text{Unif}(0, 1)$ distribution, instead of modelling ψ as a function of the joint intensity function as described in Section 2.1.1.

We obtained an independent dataset on breeding chronology from a hunter check station at the Everglades Wildlife Management Area in Miami-Dade County, Florida (Florida Fish and Wildlife Conservation Commission, unpublished data). The dataset was comprised of measurements of 54 fetuses from does harvested between 1980 and 1988. Fetal measurements were used to estimate the birth date distribution, which we compared to estimates from our model (Supporting Information S4).

In other parts of the southeastern United States, white-tailed deer mortality rates are often the highest immediately after birth and decrease with age (Nelson, Cherry, Howze, Warren, & Conner, 2015; Shuman et al., 2017). We therefore fit a model with a Weibull lifetime distribution, expecting $\omega_0 < 1$, which would indicate that the hazard decreases with age. We compared the Weibull model to an exponential model, which implicitly assumes that $\omega_0 = 1$ such that the hazard does not depend on age.

As with survival, we expected detection rates to change with age because fawns become increasingly mobile after birth. Specifically, we expected home range size to increase towards an asymptote representing the home range size of the attending doe. We therefore modelled the scale parameter of the detection function as $\sigma_i(t) = \sigma_0 \exp(-\sigma_1/a_i(t))$ where σ_0 is the asymptote and σ_1 determines the rate at which home range size increases with age. This age-specific scale parameter was included in a Gaussian encounter rate (intensity) function: $\lambda(\boldsymbol{s}_i, \boldsymbol{x}_j, t) = \lambda_0 \exp(-\|\boldsymbol{s}_i - \boldsymbol{x}_j\|^2/(2\sigma_i(t)^2))z_i(t)$ that served as the basis of the observation model. An important note about this encounter model is that it implies that $\boldsymbol{s}_i$ is the birth location, not simply the individual's activity centre, which is the typical definition of $\boldsymbol{s}_i$ in other SCR applications. The reason for this is that $\sigma_i(t)$ is close to zero immediately after birth, and therefore any individual detected at a young age must be close to its birth site. More generally, "age at detection" provides information about where the individual was born, unless individuals systematically move away from birth sites as they age.

To simplify model fitting, we discretized the model by rounding birth times down and lifetimes up to the nearest day. We then approximated the temporal Poisson point process model by modelling the encounter frequencies as Poisson random variables with expectation $\lambda_k(\boldsymbol{s}_i, \boldsymbol{x}_j)$: $k = 1, 2, \ldots, K$ where K is the number of days in the study. A few cameras failed for short amounts of time, which we accounted for by setting the encounter rate to zero in these instances.

We used uniform priors for λ_0, σ_0, σ_1, $\bar{t}$, ς, ω_0, ω_1, and ψ. After trying values of 50 and 100, we settled on $M = 150$ for data augmentation because the posterior probability $\Pr(B = 150)$ was approximately zero. We ran 8 parallel chains for 72,000 iterations, discarding the first 2,000 as burn-in. Gelman–Rubin diagnostic statistics and visual inspections were used to assess convergence. The model was fitted using a custom Gibbs sampler written in R-3.3.0 (R Core Team, 2016). Details about the joint posterior distribution, the Gibbs sampler, and R code are provided in Supporting Information S2. Point estimates reported below are posterior medians unless indicated otherwise.

3.3 | Results

We obtained 1,454 photos of 28 spotted fawns at our 60 cameras trap locations. Cameras were operational for 12,631 (98.8%) of the 12,780 possible camera days. Detections of a fawn within one hour of a previous detection at the same camera were deemed nonindependent. The one hour threshold was supported by visual inspections of histograms for the thinned and unthinned data, and by the Kolmogorov–Smirnov tests, which resulted in p-values > 0.05 for each of the 51 combinations of fawns and cameras with at least 3 detections (Supporting Information S1). After discarding these detections, we were left with 254 independent detections for our analysis (Figure 3).

The first detection occurred on January 22, 2016, more than a month and a half into the study period. The median number of independent detections of each fawn was 7 with a range of 1–30

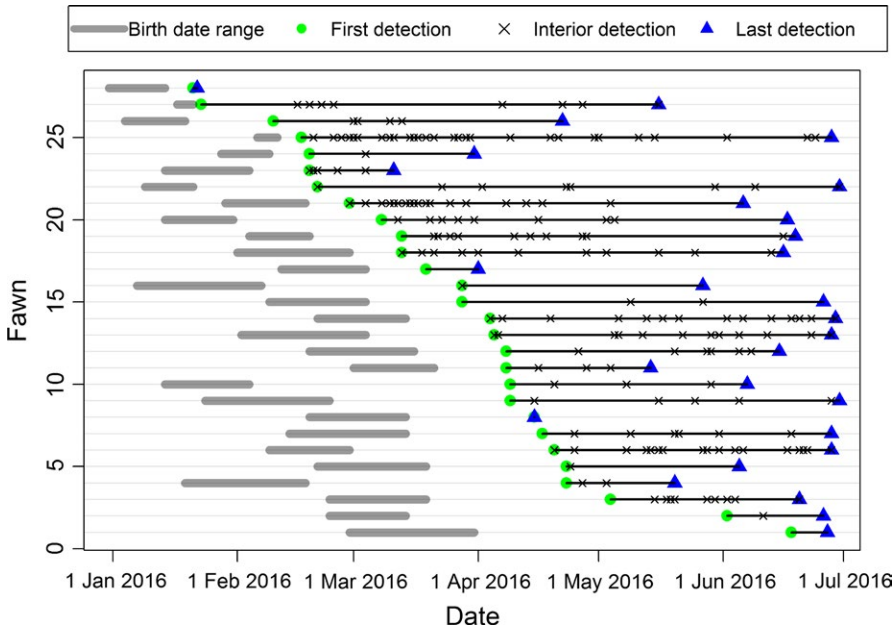

FIGURE 3 Temporal summary statistics and birth date ranges for the 28 fawns detected between December 1, 2015 and July 1, 2016. Birth date ranges were assigned by photo interpreters as described in the text

(Figure 3). Twenty seven of the 28 fawns were detected on more than one occasion. Twelve individuals were detected at a single location, 13 were detected at 2 locations, one was detected at 3 locations, and two were detected at 5 locations. The median width of the birth date intervals was 21.2 days with a range of 4–31 days (Figure 3). We never detected more than one fawn in a single image, suggesting that does rarely gave birth to twins in our study area.

Gelman–Rubin statistics were <1.1 for all parameters and visual inspections of the traceplots indicated that the Markov chains successfully converged (Supporting Information S3). The model with the Weibull lifetime distribution had one more parameter than the exponential model, yet the Weibull model did not explain any additional variation in the data as indicated by the posterior deviance. The estimate of the Weibull shape parameter was 0.61, but the 95% CI was wide and included 1 (Table 1), indicating that the data do not support the hypothesis that the hazard rate changed with age. For these reasons, we chose the exponential model as the most parsimonious model, and the results presented below, as well as Figures 4–8, are based on this model. Posterior summaries from both models are presented in Table 1, which indicates that the two models yielded similar inferences. The only substantial difference is the wider 95% CI for the number of births from the Weibull model compared to the exponential model (Table 1).

An estimated 37 (95% CI: 30–49) fawns were born in the 37.73 km^2 study area during the 2016 fawning season (Table 1). The mean birth date was February 14 (95% CI: February 6–February 22) (Table 1), and most births occurred during the first 3 months of the year (Figure 4). The estimate of mean birth date from the independent breeding chronology study was February 19 (*SE* = 2.90, Supporting Information S4).

The scale parameter (ω_1) of the exponential distribution can be interpreted as the mean lifetime, and was estimated to be 237.1 days (95% CI: 119.5–625.8, Table 1). With a constant hazard rate of $1/\omega_1$, the estimated survivorship curve predicts that 46.0% (95% CI: 22.7–74.0%) of fawns survive 180 days (Figure 5). The estimate of the realized number of recruits was 16 (95% CI: 10–23, Table 1), representing 43% of the estimated 37 fawns that were born.

The prolonged birthing season and the constant mortality rates resulted in a steep increase in fawn abundance followed by a gradual decrease in abundance after the parturition season (Figure 6). Fawn abundance peaked at 30 (95% CI: 26–35) individuals in mid-March, followed by a peak of 12 (95% CI: 3–20) recruits in mid-September. The peak of 14 recruits is lower than the 16 that were estimated to reach the recruitment age because not all 16 recruited fawns were alive at the same time. It is important to recognize that abundance estimates after June 30 (the last day of the study) are posterior predictions computed from the estimated lifetimes. This explains why the 95% CIs increase with time (Figure 6). We did not use data after June 30 because the spots of many fawns began to fade later in the summer and we did not want to model the spot loss process.

Although we did not attempt to model effects of habitat variables on spatio-temporal variation in density, posterior density surfaces provided some indication that fawn density was the highest in the northwestern region of the study area (Figure 7). There was no evidence that the timing of birth depended on location. For instance, several of the earliest births occurred in the northwestern and southeastern regions of the study area. This supports our decision to model birth time and location independently, but it does not rule out the possibility that habitat variables may influence the birth and mortality processes that determine fawn density.

Home range size increased with age, as indicated by the rapid increase in σ following birth (Figure 8). For the first few days after birth, the encounter rate was approximately zero beyond 5 m from

TABLE 1 Posterior summary statistics (Mean, *SD*, and quantiles) from the spatio-temporal models of fawn recruitment fitted to the camera data. The mean birth date represents the number of days after December 1, 2015. Lifetime was measured in days. The area to which the birth and recruitment estimates apply is 37.73 km^2. The exponential (Exp) model was deemed more parsimonious than the Weibull (Weib) model because the former had one less parameter and similar posterior deviance

Model	Parameter	Mean	*SD*	2.5%	50%	97.5%
Exp	Baseline encounter rate (λ_0)	0.12	0.014	0.094	0.12	0.15
Weib		0.12	0.014	0.094	0.12	0.15
Exp	Asymptote of σ (σ_0)	291.0	19.1	256.6	290.2	331.6
Weib		289.4	19.1	255.4	288.3	329.8
Exp	Rate at which σ increases with age (σ_1)	12.43	2.87	7.44	12.24	18.62
Weib		12.12	2.89	7.13	11.90	18.27
Exp	Mean birth date ($\bar{t}$)	76.65	4.05	68.81	76.63	84.66
Weib		76.55	3.94	68.88	76.54	84.43
Exp	Birth date *SD* (ς)	20.33	2.83	15.29	20.13	26.39
Weib		20.10	2.72	15.22	19.93	25.80
Exp	Shape parameter of lifetime distribution (ω_0)	1.00	0.00	1.00	1.00	1.00
Weib		0.77	0.55	0.16	0.61	2.23
Exp	Scale parameter of lifetime distribution (ω_1)	273.5	141.3	119.5	237.1	625.8
Weib		566.8	826.0	45.4	258.2	3,511.4
Exp	Births (*B*)	37.40	4.74	30	37	49
Weib		44.87	15.13	30	41	84
Exp	Recruits (*R*)	16.34	3.43	10	16	23
Weib		17.96	4.24	9	18	25
Exp	Deviance	2,087.2	16.69	2,056.1	2,086.5	2,121.2
Weib		2,090.7	17.4	2,058.5	2,090.0	2,126.6

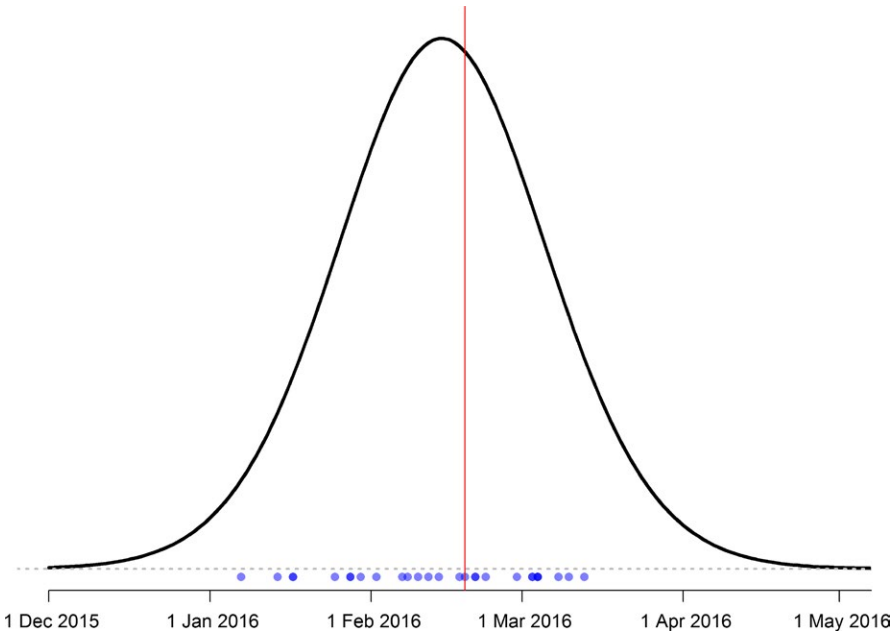

FIGURE 4 Estimates of individual birth dates (blue dots below the *x*-axis) for the 28 detected fawns, and the birth date distribution characterizing the birth dates for all (detected and not detected) fawns in the population. The vertical red line is an independent estimate of the mean parturition date from fetal measurements made on 54 does harvested in Miami-Dade County, FL, USA between 2000 and 2008

the birth location (Figure 8). However, after just 10 days, fawns were detectable out to approximately 200 m from their place of birth. After approximately 50 days, fawn home range size appeared to stabilize, possibly to the home range size of the attending doe.

4 | DISCUSSION

For many species, recruitment is considered the demographic process most sensitive to environmental variation and therefore is the focus of many monitoring programmes and studies of population

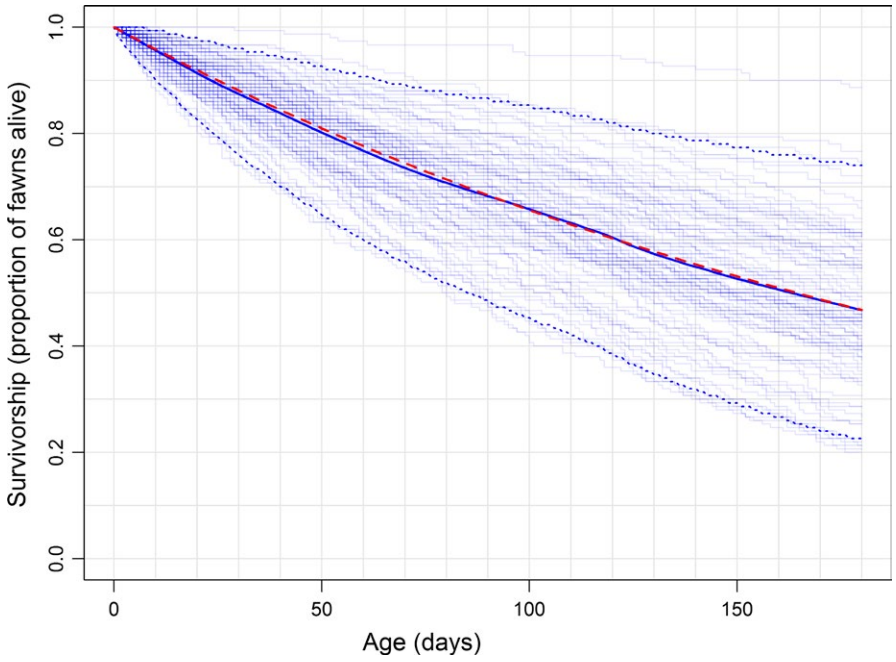

FIGURE 5 The posterior mean estimate of the realized survivorship curve (thick blue line) with 95% credible intervals (dotted blue lines). The faded lines are examples of posterior samples from which the mean and 95% CIs were computed. The dashed red line is the expected survivorship curve based on the posterior mean estimate of ω_1

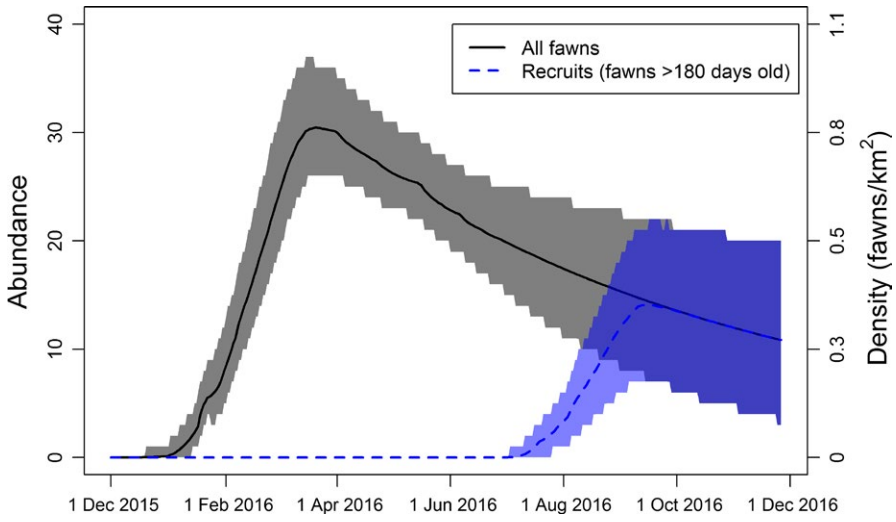

FIGURE 6 Abundance and density of all fawns and the recruited segment of the population. Shaded polygons are 95% CIs. Note that data collection ended on June 30, 2016, and estimates after that date are posterior predictions

dynamics (Clutton-Brock, Price, Albon, & Jewell, 1992; Gaillard et al., 1993; Williams et al., 2002). This is especially true for large herbivores such as deer that are typically characterized by low variation in adult survival and high variation in juvenile recruitment (Gaillard, Festa-Bianchet, & Yoccoz, 1998; Hatter & Janz, 1994; Owen-smith, 1990). We developed a model that can be used to understand the factors influencing the birth and survival processes that determine recruitment.

Our approach to recruitment modelling has numerous benefits over existing capture–recapture approaches that assume that sampling occurs at a snapshot in time. Comparing snapshot estimates of recruitment among years can result in misleading inferences if the timing of reproduction or sampling varies among years. For example, in our study, we found that four times more recruits were alive in early October than in early September, and therefore among-year comparisons would be highly sensitive to the timing of the sampling if a snapshot approach was used. Even if sampling could be conducted at the same time each year, similar problems would arise if reproductive phenology varies over time. Another advantage of our approach is that, unlike nonspatial models, our model yields estimates of recruitment per unit area. By allowing for inferences at any point in time, and within any spatial region, the modelling framework should make it easier to compare parameters among populations that were sampled using different time intervals and spatial extents. In addition, the model can accommodate age data, even when age cannot be measured exactly. This allows for inferences on age-related variation in survival and the degree to which recruitment is influenced by birth rates vs. juvenile survival. Finally, although we did not explore this option in our analysis, our model makes it possible to learn about the environmental variables influencing the timing and locations of births.

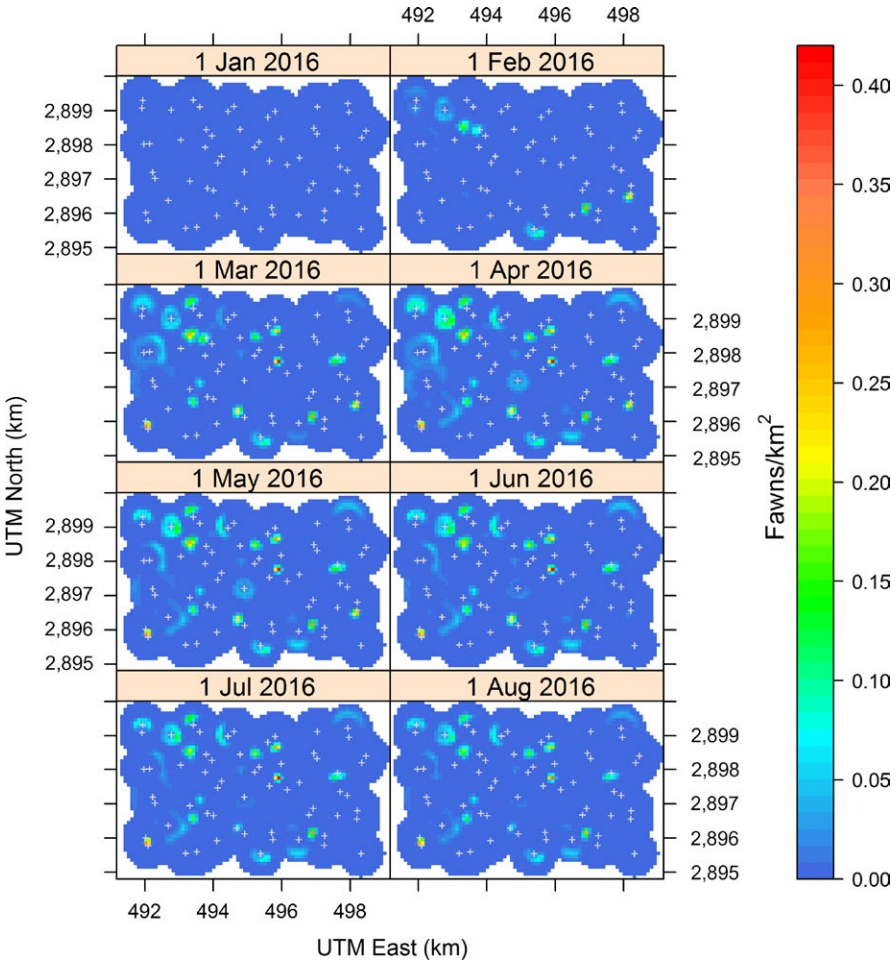

FIGURE 7 Spatiotemporal variation in the density of fawn birth sites. The 37.37 km^2 spatial region was defined by placing a 700 m buffer around the camera trap locations (white crosses). Fawn density is defined as the number of birth locations per km^2 for fawns alive at each time point. Overall fawn density and abundance are shown in Figure 6

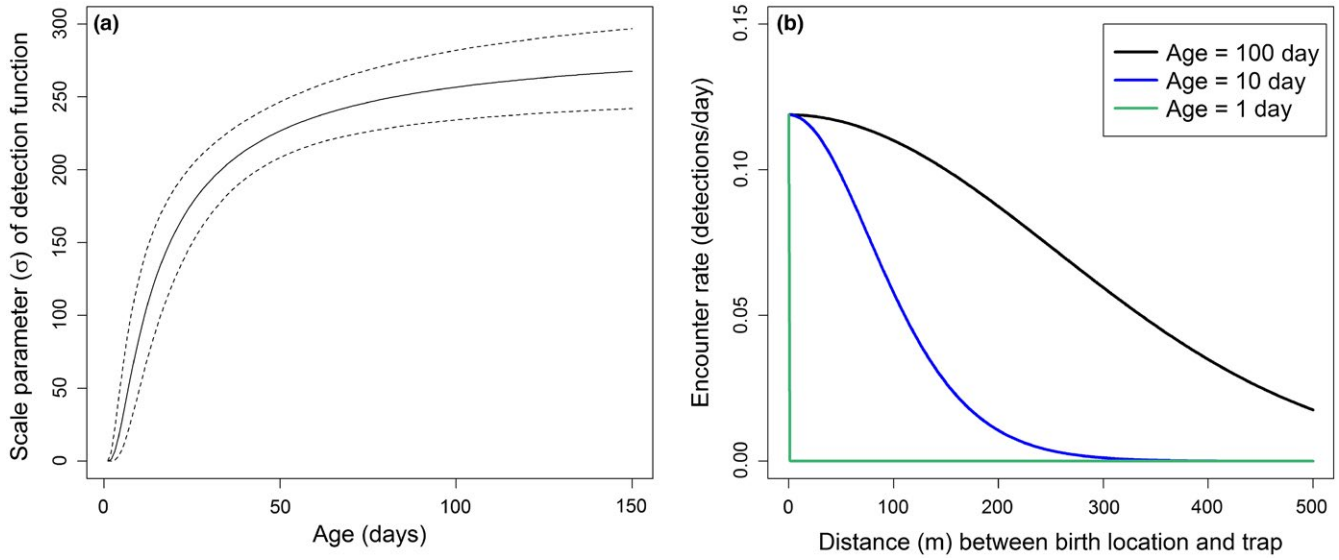

FIGURE 8 Home range size increases with age, resulting in (a) age-specific encounter rate parameters, and (b) age-specific encounter rate functions (shown for three ages)

Although capture–recapture has been the primary tool for studying recruitment in animal populations, several other approaches exist. One method involves independently estimating female abundance, fecundity, and juvenile survival. The juvenile survival component is typically accomplished using telemetry but is particularly challenging because many individuals die soon after being born, making it

difficult to study survival in that critical age range (Gilbert, Lindberg, Hundertmark, & Person, 2014). To overcome this challenge, novel technologies, such as vaginal implant transmitters, have been developed to determine when births occur so that neonates can be captured and tracked. This process can be extremely expensive, and the invasive nature of the work may impact the survival parameters of interest. Our approach is less expensive and invasive than telemetry studies. In addition, it allows for population-level inference, which is difficult to achieve in telemetry studies unless individuals can be randomly sampled or if the capture (i.e., sample inclusion) process can be modelled. The primary drawbacks of our approach are that it does not provide information about cause-specific mortality and it provides less direct information about survival than telemetry studies.

From a statistical perspective, our model can be described as either a spatial birth-death process or as a spatio-temporal point process model (Bailey, 1968; Cox & Isham, 1980; Diggle, 2013; Preston, 1975; Rathbun & Cressie, 1994). In the classification scheme of González et al. (2016) our model would be placed in the second category of spatio-temporal models, in which the points do not move over time, but instead enter and exit the state-space according to stochastic processes. However, unlike most spatio-temporal point process models in the statistical literature, we treat the state process as latent, and we use a conditional observation model—a thinning model—for the capture–recapture data. Even though not all points are observed, the observation model makes it possible to use the locations of detection and the ages of the detected individuals to probabilistically determine the birth locations and birth times. In addition, the information about lifetime comes from the encounter rate data because a high encounter rate suggests that an individual died soon after it was last detected (unless it was detected near the end of the study period). Conversely, low encounter rates suggest that an individual may have lived much longer after its last detection. With respect to existing capture–recapture models, our state model is most similar to that of Crosbie and Manly (1985), except that their model is nonspatial and does not accommodate age data. The primary differences between our model and similar open population SCR models (Gardner et al., 2010; Raabe et al., 2013) is that the latter formulate the entry and survival processes using a hidden Markov model in discrete time, and they ignore age. Under the hidden Markov approach, each $z_i(t)$ after the first time period is modelled conditional on $z_i(t-1)$, and therefore, there are T latent z variables to estimate for each individual, instead of just 2 (birth date and lifetime) as in our model. This reduces the number of latent variables that must be estimated, or integrated out of the likelihood, by a factor of $T/2$, thereby greatly reducing computation time.

Many model extensions warrant future exploration. As with most SCR models, we intentionally avoided the complexities associated with adopting an explicit movement model, which is justified given that movement is typically not the subject of inquiry in capture–recapture studies. However, there are at least three situations in which it might be useful to adopt explicit movement models within a SCR framework. The first is if movement itself is of interest (Lebreton et al., 2003; Raabe et al., 2013; Royle, Fuller, & Sutherland, 2016). For example, a movement model could be used to study the contributions of immigration to total, rather than *in situ*, recruitment. A second reason for adopting a movement model is to account for autocorrelation in detection times that might arise when detector density is high relative to the movement rate of the study species (Borchers et al., 2014). In our case, we dealt with temporal autocorrelation by discarding nonindependent photos and by allowing the scale parameter of the detection function to increase with age. Even so, it is possible that some spatial autocorrelation was still present and unaccounted for in our model, and further thinning may have resulted in an unsatisfactory number of detections. A third reason for including a movement model would be to relax the assumption of stationary home ranges. Our model assumes that encounter rate depends only on age and the distance from the birth location to the detector. However, if individuals systematically select habitat that is far from their birth locations, bias in the encounter rate parameters could arise. Future work could address these issues by adopting a movement model, such as the Ornstein–Uhlenbeck process (Hooten, Johnson, McClintock, & Morales, 2017), and then modelling detection conditional on location at time t, rather than as a function of distance to activity centre. Another extension worth considering is allowing for negative covariance between the baseline encounter rate λ_0 and the scale parameter σ, which would arise if animals spend less time near their home range centres as their home ranges expand with age (Efford & Mowat, 2014).

Several design issues should be considered when attempting to study recruitment with our model. As with most SCR studies, minimizing the variance of the recruitment estimator can be achieved by finding the spatial arrangement of detectors that results in a good balance of the number of individuals detected and the number of recaptures obtained (Sollmann, Gardner, & Belant, 2012). Although there is no optimal spacing that applies to all systems, a good design can often be achieved by using a detector spacing of approximately 2σ (Chandler & Royle, 2013). However, our model assumes that σ changes with age, indicating that the optimal detector density might also change throughout the season. Although the logistics associated with changing detector configurations during sampling could be prohibitive, it might be useful to attempt to keep detector spacing near 2σ by using high density clusters of detectors early in the season when most individuals are young, and then spreading them out into a more uniform pattern when home range sizes stabilize. This could help detect fawns at earlier ages, thereby removing some of the uncertainty about age-related variation in survival. The temporal aspect of the design is also likely to affect the precision of estimates. Intuitively, one should attempt to begin sampling before the first birth event and continue until the last recruitment event. Using data from shorter time intervals will add to the uncertainty about birth dates and survival times, but should not cause bias unless the model for the distribution of birth times is mis-specified. Although it would be impossible to fully explore these design and model considerations, we recommend conducting simulation studies in the context

of specific study objectives and constraints, and we provide some simulation code in Supporting Information.

Results from our analysis of the deer data suggested that overall fawn survival rate was comparable to telemetry-based estimates from southern Florida Florida (Land, 1991); however, unlike other recent studies of fawn survival from elsewhere in the southeastern US (Chitwood et al., 2015; Kilgo, Ray, Vukovich, Goode, & Ruth, 2012; Saalfeld & Ditchkoff, 2007; Shuman et al., 2017), mortality rates were essentially constant during the first 6 months of life, with approximately 40% of individuals surviving to the recruitment age. Strikingly, a recent study from Louisiana found that only 50% of fawns survived the first week of life, although mortality rates quickly decreased to the point that 27% of the fawns in their sample survived to 84 days (Shuman et al., 2017). We propose three hypotheses to explain the large differences in age-specific survival rates between our study area and those in other regions of the southeastern US. First, previous studies used telemetry, and it is possible that some neonatal mortality in these studies was attributable to capture, handling, and use of the transmitters themselves. Although no evidence of transmitter and handling effects exists, it would be possible to evaluate this hypothesis by using our model to compare survival rates of collared and uncollared individuals.

A second hypothesis explaining the relatively low neonate mortality that we observed concerns the unique predator community in our study area. Our work was conducted in the only region of the eastern US with a reproducing puma population. Panthers are ambush predators, and therefore may be less likely to depredate young fawns than other predators, particularly while fawns are still in the hiding phase and remain motionless for the majority of the day between feedings (Ballard, Lutz, Keegan, Carpenter, & deVos, 2001; Preisser, Orrock, & Schmitz, 2007; Schmitz, 2008, but see McCoy, Murphie, Gunther, & Murphie, 2014). In addition, deer survival studies conducted elsewhere likely had higher densities of the three major fawn predators found in the southeastern US: black bear *Ursus americanus*, bobcat *Lynx rufus*, and coyote *Canis latrans*. Coyote density is extremely low in our study area relative to other regions in the southeastern US, as coyotes have been documented in southern Florida only within the last few decades (McCown & Scheick, 2007). Black bears can be effective fawn predators within the first few weeks of life before fawns are highly mobile (Shuman et al., 2017). However, South Florida black bears are largely dormant in February during peak fawning, and predation on deer by bears in this region appears to be opportunistic and only constitutes a small portion of their diet (Maehr & Brady, 1984). Additionally, bear density in Big Cypress (0.13 bears/km^2, Humm, McCown, Scheick, & Clark, 2016) is considerably lower than in other areas of the southeastern US, such as Louisiana (0.66 bears/km^2, Hooker, 2010). Bobcats are abundant in our study area and can greatly affect fawn survival (Labisky, Boulay, Miller, Sargent, & Zultowsky, 1995; Land, 1991; Nelson et al., 2015; Shuman et al., 2017), but they are ambush predators and therefore likely do not frequently encounter sedentary neonates.

A third explanation of the lack of evidence of age-related variation in survival is that our sample size may have been too small to detect the age effect. This is suggested by the wide credible interval for the shape parameter of the Weibull distribution. The lack of precision can be attributed to detecting only 28 fawns, most of which were first detected after their second week of life. The ability to detect age effects in survival can be expected to increase with the number of individuals detected, the average encounter rate, and timespan of the study relative to the average lifetime of the species. For species such as white-tailed deer with low neonate movement rates, precision could also be increased through efforts to increase encounter rates of young fawns or by extending the model to accommodate both camera and telemetry data.

Another direction for future work is to develop better methods for aging individuals using camera data or other types of data for which age cannot be determined precisely. One option would be to conduct experiments with captive individuals to determine how morphological measurements, or perhaps ratios of measurements, change with age when individuals are detected at variable distances and angles. Simple regression models could then be used to predict age with more precision than we achieved with our wide birth date ranges. Future work could also attempt to account for the loss of spots after fawns are 6 months old. We ignored this problem because fewer than two individuals likely reached this age during our sampling time frame (Figure 6). However, we could have extended our time frame and modelled the spot loss process by incorporating data on unmarked individuals (Chandler & Royle, 2013).

Birth site locations were assumed to be mutually independent because we had no evidence of clustering or repulsion. For example, we never detected more than one fawn in a photo, and fecundity is believed to be <1.2 fawns/doe in southern Florida (Land, 1991). However, for species with higher fecundity that can give birth to multiple offspring in the same location, data on litter size could be used to model nonindependence of birth sites using a marked point process in which the mark is the number of individuals born at location $\boldsymbol{s}_i$ (Diggle, 2013). More general forms of clustering could be modelled with a Neyman–Scott process, whereas territoriality and other forms of inhibition could be modelled with a Markov point process (Reich & Gardner, 2014).

Our model could also be extended to include multiple age classes, which would allow for inferences about fecundity. In our analysis, we ignored the adult portion of the population and directly estimated the number of births per unit area. This was deliberate because adult female deer typically cannot be uniquely identified, making it difficult to estimate their abundance. However, if adult abundance could be estimated, perhaps by using recently developed methods for unmarked animals (Chandler & Royle, 2013), the expected number of births could be modelled using a density-dependent fecundity function. Although this would increase the complexity of the model, it might result in more precise estimates of birth and recruitment parameters. More importantly, it would provide a means of connecting SCR models to classical age-structured population models and integral projection models, which are rarely formulated as spatially explicit statistical models (Caswell, 2001; Ellner & Rees, 2006).

ACKNOWLEDGEMENTS

Daniel Crawford and Brian Kelly helped oversee field operations. Caitlin Kupar assisted with data collection, and Michael Biggerstaff assisted with aging individuals. We thank Cory Morea for discussions regarding study objectives and fawn survival. Funding was provided by the Florida Fish and Wildlife Conservation Commission. Housing and logistical support was provided by the US Fish and Wildlife Service. Access to our study area was granted by the US National Park Service.

AUTHORS' CONTRIBUTIONS

R.B.C., M.J.C., E.P.G. and K.V.M. designed the study. K.E. assisted with data collection and analysis. R.B.C. led the analysis and wrote the first draft of the manuscript. All authors edited the manuscript.

DATA ACCESSIBILITY

Data and code are available at https://github.com/rbchan/mee-fawn-data, https://doi.org/10.5281/zenodo.1317453.

ORCID

Richard B. Chandler http://orcid.org/0000-0003-4930-2790

REFERENCES

Bailey, N. T. (1968). Stochastic birth, death and migration processes for spatially distributed populations. *Biometrika*, *55*, 189–198. https://doi.org/10.2307/2334463

Ballard, W. B., Lutz, D., Keegan, T. W., Carpenter, L. H., & deVos Jr, J. C. (2001). Deer-predator relationships: A review of recent North American studies with emphasis on mule and black-tailed deer. *Wildlife Society Bulletin*, *29*, 99–115.

Borchers, D. L., & Efford, M. (2008). Spatially explicit maximum likelihood methods for capture–recapture studies. *Biometrics*, *64*, 377–385. https://doi.org/10.1111/j.1541-0420.2007.00927.x

Borchers, D., Distiller, G., Foster, R., Harmsen, B., & Milazzo, L. (2014). Continuous-time spatially explicit capture–recapture models, with an application to a jaguar camera-trap survey. *Methods in Ecology and Evolution*, *5*, 656–665. https://doi.org/10.1111/2041-210x.12196

Caswell, H. (2001). *Matrix population models*. Sunderland, MA: Sinauer.

Chandler, R. B., & Royle, J. A. (2013). Spatially explicit models for inference about density in unmarked or partially marked populations. *Annals of Applied Statistics*, *7*, 936–954. https://doi.org/10.1214/12-aoas610

Chitwood, M. C., Lashley, M. A., Kilgo, J. C., Pollock, K. H., Moorman, C. E., & DePerno, C. S. (2015). Do biological and bedsite characteristics influence survival of neonatal white-tailed deer? *PLoS ONE*, *10*, e0119070. https://doi.org/10.1371/journal.pone.0119070

Chitwood, M. C., Lashley, M. A., Kilgo, J. C., Cherry, M. J., Conner, L. M., Vukovich, M., … Moorman, C. E. (2017). Are camera surveys useful for assessing recruitment in white-tailed deer? *Wildlife Biology*, *2017*, wlb.00178. https://doi.org/10.2981/wlb.00178

Clutton-Brock, T., Price, O., Albon, S., & Jewell, P. (1992). Early development and population fluctuations in Soay sheep. *Journal of Animal Ecology*, *61*, 381–396. https://doi.org/10.2307/5330

Cox, D. R., & Isham, V. (1980). *Point processes*, *vol. 12 of Monographs on applied probability and statistics*. London: Chapman and Hall, Ltd.

Cox, D. R., & Oakes, D. (1984). *Analysis of survival data*, vol. 21. Boca Raton, FL: CRC Press.

Crosbie, S., & Manly, B. (1985). Parsimonious modelling of capture-mark-recapture studies. *Biometrics*, *41*, 385–398. https://doi.org/10.2307/2530864

Diggle, P. J. (2013). *Statistical analysis of spatial and spatio-temporal point patterns*. Boca Raton, FL: CRC Press.

Dorazio, R. M., & Karanth, K. U. (2017). A hierarchical model for estimating the spatial distribution and abundance of animals detected by continuous-time recorders. *PLoS ONE*, *12*, e0176966. https://doi.org/10.1371/journal.pone.0176966

Efford, M. (2004). Density estimation in live-trapping studies. *Oikos*, *106*, 598–610. https://doi.org/10.1111/j.0030-1299.2004.13043.x

Efford, M., & Mowat, G. (2014). Compensatory heterogeneity in spatially explicit capture–recapture data. *Ecology*, *95*, 1341–1348. https://doi.org/10.1890/13-1497.1

Ellner, S. P., & Rees, M. (2006). Integral projection models for species with complex demography. *American Naturalist*, *167*, 410–428. https://doi.org/10.2307/3844763

Gaillard, J. M., Delorme, D., Boutin, J. M., Van Laere, G., Boisaubert, B., & Pradel, R. (1993). Roe deer survival patterns: A comparative analysis of contrasting populations. *Journal of Animal Ecology*, *62*, 778–791. https://doi.org/10.2307/5396

Gaillard, J. M., Festa-Bianchet, M., & Yoccoz, N. G. (1998). Population dynamics of large herbivores: Variable recruitment with constant adult survival. *Trends in Ecology & Evolution*, *13*, 58–63. https://doi.org/10.1016/s0169-5347(97)01237-8

Gardner, B., Reppucci, J., Lucherini, M., & Royle, J. A. (2010). Spatially explicit inference for open populations: Estimating demographic parameters from camera-trap studies. *Ecology*, *91*, 3376–3383. https://doi.org/10.1890/09-0804.1

Gilbert, S. L., Lindberg, M. S., Hundertmark, K. J., & Person, D. K. (2014). Dead before detection: Addressing the effects of left truncation on survival estimation and ecological inference for neonates. *Methods in Ecology and Evolution*, *5*, 992–1001. https://doi.org/10.1111/2041-210x.12234

Godsoe, W., Jankowski, J., Holt, R. D., & Gravel, D. (2017). Integrating biogeography with contemporary niche theory. *Trends in Ecology & Evolution*, *32*, 488–499. https://doi.org/10.1016/j.tree.2017.03.008

González, J. A., Rodríguez-Cortés, F. J., Cronie, O., & Mateu, J. (2016). Spatio-temporal point process statistics: A review. *Spatial Statistics*, *18*, 505–544. https://doi.org/10.1016/j.spasta.2016.10.002

Gurevitch, J., Fox, G. A., Fowler, N. L., Graham, C. H., & Thomson, J. D. (2016). Landscape demography: Population change and its drivers across spatial scales. *Quarterly Review of Biology*, *91*, 459–485. https://doi.org/10.1086/689560

Hatter, I. W., & Janz, D. W. (1994). Apparent demographic changes in black-tailed deer associated with wolf control on northern Vancouver Island. *Canadian Journal of Zoology*, *72*, 878–884. https://doi.org/10.1139/z94-119

Hooker, M. J. (2010). Estimating population parameters of the Louisiana black bear in the Tensas River Basin, Louisiana, using robust design capture-mark-recapture. Master's thesis, University of Tennessee.

Hooten, M., Johnson, D., McClintock, B., & Morales, J. (2017). *Animal movement: Statistical models for telemetry Data*. Boca Raton, FL: Chapman & Hall/CRC.

Humm, J., McCown, J. W., Scheick, B. K., & Clark, J. D. (2016). Black bear population size and density in Apalachicola, Big Cypress, Eglin, Ocala/St. Johns, and Osceola Study Areas, Florida. Department of

Forestry, Wildlife and Fisheries, University of Tennessee. Final report to Florida Fish and Wildlife Commission.

Jolly, G. M. (1965). Explicit estimates from capture–recapture data with both death and immigration-stochastic model. *Biometrika*, *52*, 225–247. https://doi.org/10.2307/2333826

Kilgo, J. C., Ray, H. S., Vukovich, M., Goode, M. J., & Ruth, C. (2012). Predation by coyotes on white-tailed deer neonates in South Carolina. *Journal of Wildlife Management*, *76*, 1420–1430. https://doi.org/10.1002/jwmg.393

Labisky, R. F., Boulay, M. C., Miller, K. E., Sargent, R. A., & Zultowsky, J. M. (1995). Population ecology of white-tailed deer in Big Cypress National Preserve and Everglades National Park. Department of Wildlife Ecology and Conservation, University of Florida. Final Report to USDI.

Land, D. E. (1991). Big cypress deer/panther relationships: Deer mortality. Bureau of Wildlife Research, Florida Game and Fresh Water Fish Commission. Final Report, Study Number: 7509.

Lebreton, J., Hines, J., Pradel, R., Nichols, J., & Spendelow, J. (2003). Estimation by capture–recapture of recruitment and dispersal over several sites. *Oikos*, *101*, 253–264. https://doi.org/10.1034/j.1600-0706.2003.11848.x

Maehr, D. S., & Brady, J. R. (1984). Food habits of Florida black bears. *Journal of Wildlife Management*, *48*, 230–235. https://doi.org/10.2307/3808478

Matechou, E., Pledger, S., Efford, M., Morgan, B. J., & Thomson, D. L. (2013). Estimating age-specific survival when age is unknown: Open population capture–recapture models with age structure and heterogeneity. *Methods in Ecology and Evolution*, *4*, 654–664. https://doi.org/10.1111/2041-210x.12061

McCown, W., & Scheick, B. (2007). The Coyote in Florida. Fish and Wildlife Research Institute, Florida Fish and Wildlife Conservation Commission.

McCoy, R. H., Murphie, S. L., Gunther, M. S., & Murphie, B. L. (2014). Influence of hair loss syndrome on black-tailed deer fawn survival. *The Journal of Wildlife Management*, *78*, 1177–1188. https://doi.org/10.1002/jwmg.772

Merow, C., Latimer, A. M., Wilson, A. M., McMahon, S. M., Rebelo, A. G., & Silander, J. A. (2014). On using integral projection models to generate demographically driven predictions of species' distributions: Development and validation using sparse data. *Ecography*, *37*, 1167–1183. https://doi.org/10.1111/ecog.00839

Nelson, M. A., Cherry, M. J., Howze, M. B., Warren, R. J., & Conner, L. M. (2015). Coyote and bobcat predation on white-tailed deer fawns in a longleaf pine ecosystem in southwestern Georgia. *Journal of the Southeastern Association of Fish and Wildlife Agencies*, *2*, 208–213.

Nichols, J. D., & Pollock, K. H. (1990). Estimation of recruitment from immigration versus in situ reproduction using Pollock's robust design. *Ecology*, *71*, 21–26. https://doi.org/10.2307/1940243

Owen-smith, N. (1990). Demography of a large herbivore, the greater kudu *Tragelaphus strepsiceros*, in relation to rainfall. *Journal of Animal Ecology*, *59*, 893–913. https://doi.org/10.2307/5021

Pollock, K. H. (1981). Capture–recapture models allowing for age-dependent survival and capture rates. *Biometrics*, *37*, 521–529. https://doi.org/10.2307/2530565

Pollock, K. H. (1982). A capture–recapture design robust to unequal probability of capture. *Journal of Wildlife Management*, *46*, 752–757. https://doi.org/10.2307/3808568

Pradel, R. (1996). Utilization of capture-mark-recapture for the study of recruitment and population growth rate. *Biometrics*, *52*, 703–709. https://doi.org/10.2307/2532908

Pradel, R., & Lebreton, J. D. (1999). Comparison of different approaches to the study of local recruitment of breeders. *Bird Study*, *46*, S74–S81. https://doi.org/10.1080/00063659909477234

Preisser, E. L., Orrock, J. L., & Schmitz, O. J. (2007). Predator hunting mode and habitat domain alter nonconsumptive effects in predator-prey interactions. *Ecology*, *88*, 2744–2751. https://doi.org/10.1890/07-0260.1

Preston, C. (1975). Spatial birth and death processes. *Advances in Applied Probability*, *7*, 465–466. https://doi.org/10.1017/s0001867800040726

R Core Team. (2016). *R: A language and environment for statistical computing*. Vienna, Austria: R Foundation for Statistical Computing. https://www.R-project.org/

Raabe, J. K., Gardner, B., & Hightower, J. E. (2013). A spatial capture–recapture model to estimate fish survival and location from linear continuous monitoring arrays. *Canadian Journal of Fisheries and Aquatic Sciences*, *71*, 120–130. https://doi.org/10.1139/cjfas-2013-0198

Rathbun, S. L., & Cressie, N. (1994). A space-time survival point process for a longleaf pine forest in southern Georgia. *Journal of the American Statistical Association*, *89*, 1164–1174. https://doi.org/10.2307/2290979

Reich, B. J., & Gardner, B. (2014). A spatial capture–recapture model for territorial species. *Environmetrics*, *25*, 630–637. https://doi.org/10.1002/env.2317

Royle, J. A. (2009). Analysis of capture–recapture models with individual covariates using data augmentation. *Biometrics*, *65*, 267–274. https://doi.org/10.1111/j.1541-0420.2008.01038.x

Royle, J. A., Dorazio, R. M., & Link, W. A. (2007). Analysis of multinomial models with unknown index using data augmentation. *Journal of Computational and Graphical Statistics*, *16*, 67–85. https://doi.org/10.1198/106186007x181425

Royle, J. A., Chandler, R. B., Sollmann, R., & Gardner, B. (2014). *Spatial capture–recapture*. Waltham, MA: Academic Press.

Royle, J. A., Fuller, A. K., & Sutherland, C. (2016). Spatial capture–recapture models allowing Markovian transience or dispersal. *Population Ecology*, *58*, 53–62. https://doi.org/10.1007/s10144-015-0524-z

Saalfeld, S. T., & Ditchkoff, S. S. (2007). Survival of neonatal white-tailed deer in an exurban population. *Journal of Wildlife Management*, *71*, 940–944. https://doi.org/10.2193/2006-116

Sanderlin, J. S., Waser, P. M., Hines, J. E., & Nichols, J. D. (2012). On valuing patches: Estimating contributions to metapopulation growth with reverse-time capture–recapture modelling. *Proceedings of the Royal Society of London B: Biological Sciences*, *279*, 480–488. https://doi.org/10.1098/rspb.2011.0885

Schaub, M., & Royle, J. A. (2014). Estimating true instead of apparent survival using spatial Cormack–Jolly–Seber models. *Methods in Ecology and Evolution*, *5*, 1316–1326. https://doi.org/10.1111/2041-210x.12134

Schaub, M., Ullrich, B., Knötzsch, G., Albrecht, P., & Meisser, C. (2006). Local population dynamics and the impact of scale and isolation: A study on different little owl populations. *Oikos*, *115*, 389–400. https://doi.org/10.1111/j.2006.0030-1299.15374.x

Schmitz, O. J. (2008). Effects of predator hunting mode on grassland ecosystem function. *Science*, *319*, 952–954. https://doi.org/10.1126/science.1152355

Schwarz, C. J., & Arnason, A. N. (1996). A general methodology for the analysis of capture–recapture experiments in open populations. *Biometrics*, *52*, 860–873. https://doi.org/10.2307/2533048

Seber, G. A. (1965). A note on the multiple-recapture census. *Biometrika*, *52*, 249–259. https://doi.org/10.1093/biomet/52.1-2.249

Shuman, R. M., Cherry, M. J., Simoneaux, T. N., Dutoit, E. A., Kilgo, J. C., Chamberlain, M. J., & Miller, K. V. (2017). Survival of white-tailed deer neonates in Louisiana. *Journal of Wildlife Management*, *81*, 834–845. https://doi.org/10.1002/jwmg.21257

Sollmann, R., Gardner, B., & Belant, J. L. (2012). How does spatial study design influence density estimates from spatial capture–recapture models? *PLoS ONE*, *7*, e34575. https://doi.org/10.1371/journal.pone.0034575

Stokes, S. L. (1984). The Jolly-Seber method applied to age-stratified populations. *Journal of Wildlife Management*, *48*, 1053–1059. https://doi.org/10.2307/3801468

USFWS. (2017). Mourning dove harvest strategy 2017. U.S. Fish and Wildlife Service, Washington, D.C.

Williams, B. K., Nichols, J. D., & Conroy, M. J. (2002). *Analysis and management of animal populations*. San Diego, CA: Academic Press.

SUPPORTING INFORMATION

Additional supporting information may be found online in the Supporting Information section at the end of the article.

How to cite this article: Chandler RB, Engebretsen K, Cherry MJ, Garrison EP, Miller KV. Estimating recruitment from capture–recapture data by modeling spatio-temporal variation in birth and age-specific survival rates.
Methods Ecol Evol. 2018;9:2115–2130.
https://doi.org/10.1111/2041-210X.13068